

Angular distributions of dissociation fragments from low-kilovolt-energy collisions of H_2^+ on He

I. Alvarez and C. Cisneros

Instituto de Física, Universidad Nacional Autónoma de México, Mexico 20, D.F.

A. Russek

The University of Connecticut, Storrs, Connecticut 06268

(Received 2 September 1980)

Differential cross sections are presented for the production of H^+ and H^0 fragments produced in collisions of H_2^+ with He at collision energies 0.5, 1.0, 2.0, and 3.0 keV. The results are interpreted in terms of direct collisional excitation of the $1\sigma_u$ repulsive state of H_2^+ and charge exchange into the $^3\Sigma_u$ repulsive state of H_2^0 . The angular distributions of H^0 fragments which arise from the H_2^0 repulsive state are given by the angular distribution for $(1/2)(H^0 - H^+)$. The results are in agreement with those of previous experiments and extend the earlier work down to lower collision energies. The measured angular distributions fit a scaling law $(1/E_{inc})d\sigma/d\omega = N(E_{inc})f_i(E_{inc}\theta^2)$, where i indicates the dissociation fragment.

I. INTRODUCTION

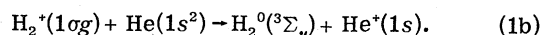
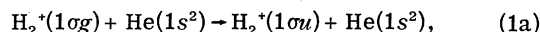
In a previous work,¹ it was seen that information could be obtained about the electronic states (both ground and excited) of the triatomic molecular collision complex $(H_2X)^+$ by examining the angular distributions of H^+ , H^0 , and H^- dissociation fragments produced in low keV energy collisions of H_2^+ on X. These collisions are sufficiently slow to be electronically adiabatic, or near adiabatic, and therefore probe the adiabatic electronic states. At the same time, the collisions are sufficiently fast that negligible rotational or vibrational motion of the incident H_2^+ ion takes place during the collision time. Consequently, the dissociation energy of the H_2 molecule or ion, which can be inferred from the angular distribution of dissociation fragments, determines the proton-proton separation at the time of collision.

However, the study of Ref. 1 was restricted to D_2^+ on Cs collisions, motivated by the search for efficient D^- production for injection heating of a fusion plasma. The realization that the electronic energy states of the triatomic molecular collision complex were being probed came only after the fact. We have been motivated to employ the technique to study collisions of H_2^+ on He. The energy surfaces of the $(H_2He)^+$ triatomic molecular ion are readily accessible to *ab initio* computations, and it is hoped that existing experimental results will provide theorists with an impetus to make the relevant calculations.

The present experiment measured angular distributions of H^+ and H^0 dissociation fragments from collisions of H_2^+ with He at collision energies of 0.5, 1.0, 2.0, and 3.0 keV. Both direct excitation of H_2^+ to repulsive states and charge exchange to repulsive states of H_2^0 were studied. In

earlier experiments, Gibson and Los² described an experimental technique whereby both orientation and internuclear separation of the H_2^+ at the time of excitation is obtained from a simultaneous measurement of velocity and angle of the H^+ dissociation fragment. The method was used by Gibson, Los, and Shopman³ to study collisional excitation of H_2^+ to dissociating states in H_2^+ on He collisions at collision energies of 3.0, 5.0, 7.5, and 10.0 keV. That technique cannot, however, be used to study charge-exchange excitation to repulsive states of H_2^0 . Sauers, Fitzwilson, Ford, and Thomas⁴ measured angular distributions for both H^+ and H^0 dissociation fragments in H_2^+ on He collisions with an experimental arrangement basically similar to the present one. However, their collision energies were higher (4.0, 5.0, 8.0, and 12.0 keV) and they were unable to measure distributions at small angles.

In collisions of H_2^+ on He, the important repulsive states involved are the $H_2^+(1\sigma_u)$ state produced by direct excitation, and the $H_2^0(^3\Sigma_u)$ state produced in a single electron-capture collision:



Cross sections for processes leading to H^- are small, and can be neglected in comparison with processes (1a) and (1b). Both H^+ and H^0 fragments were found in the experiment, and at angles with respect to the incident-beam direction attesting to considerable dissociation energy. From the relative numbers of neutral and positive ion fragments, the relative cross sections for both direct and charge-exchange excitation processes (1a) and (1b) have been established as functions of collision energy. The fact that these excitation

processes occur at such low relative velocities clearly indicates the existence of energy surface intersections in the triatomic molecular ion (the analog of curve crossings in a diatomic system).

The following section describes the apparatus and experimental procedure. Section III briefly reviews the theory of the angular distributions and the scaling law of Ref. 1. In Sec. IV, the experimental data are presented and replotted in terms of scaled variables. The cross sections for direct and charge-exchange excitation as functions of collision energy are deduced.

II. APPARATUS AND MEASUREMENTS

A. General description

The apparatus shown in Fig. 1 consists basically of three parts: ion source, scattering chamber, and detection system. The scattering chamber and detection system used in this work were similar to those described in Ref. 5. H_2^+ ions were produced in a colutron type ion source⁶ containing a mixture of 75%, 99.99% pure H_2 gas and 25% Ar for enhanced ion production.⁷ Ions were extracted and focused by an Einzel-type lens and directed to a Wien⁶ velocity filter in order to obtain mass analyzed H_2^+ ions at the desired velocity. The ions passed between cylindrical electrostatic deflection plates which were used both to steer the beam and also to bend it 10° to prevent photons from the ion source reaching the detection system. The velocity selected, mass analyzed H_2^+ entered the He interaction cell, a cylinder 2.5 cm long and 2.5 cm in diameter in which the target gas pressure was measured with a calibrated mks capacitance manometer. The molybdenum entrance aperture was 1 mm in diameter; the exit slit was 2 mm wide and 6 mm long. This geometry permitted the measurement of dissociation fragments,

the directions of which make an angle of up to $\pm 7^\circ$ with respect to the incoming beam direction.⁸ Path lengths and apertures were chosen such that the root-mean-square angular resolution of the system was 0.1° . The detector assembly rotated about the center of the gas cell so that angular distributions could be obtained. The detection system was the same as that described previously.^{1,5} The H^+ and H^0 dissociation fragments, separated by a 45° parabolic electrostatic analyzer,⁹ were counted by funnel-type channel electron multipliers. The multiplier counting efficiency for H^+ has been determined previously¹⁰ and the efficiency for H^0 was assumed to be the same as H^+ at the same energy. All experimental data have been corrected for counting efficiency.

B. Procedure

The procedure was the same as that described in Ref. 1. The incident intensity I_{inc} (the number of H_2^+ ions incident per unit area per sec) was monitored by the Faraday cup; the H^+ and H^0 ($I_+(\theta)$, $I_0(\theta)$) fragments contained in the solid angle $\Delta\omega$ at angle θ were determined as functions of θ , as the detection assembly was rotated about the He cell; the number of He atoms per unit volume was determined by the gas target density. With these measurements, the quantity

$$\frac{d\sigma_f}{d\omega} = \frac{I_f(\theta)}{I_{inc}} \quad (2)$$

was calculated, where f stands either for H^+ or the combined neutral component ($H^0 + H_2^0$). The detector was not capable of discriminating between H^0 and H_2^0 . However, it can confidently be expected that any H_2^0 present will only be found at small angles, less than 1° . Hard scattering, when it occurs, will at the same time dissociate the H_2^0 into its components. Moreover, the cross

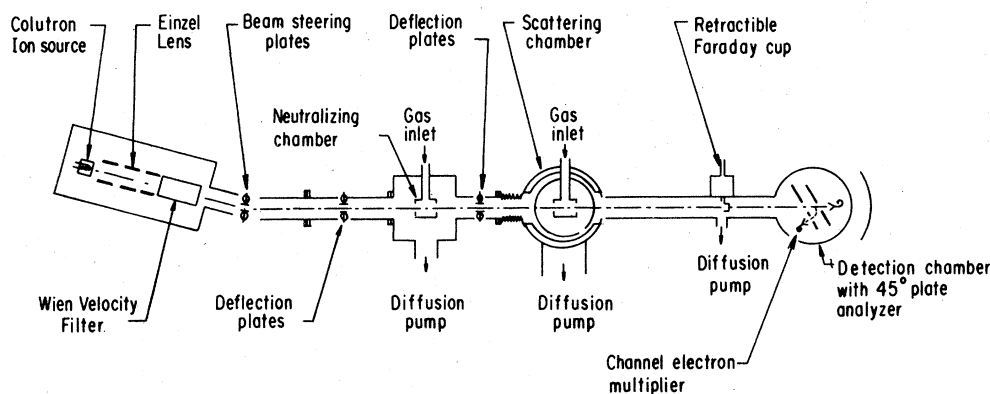


FIG. 1. Schematic diagram of the apparatus.

section for hard scattering is very small compared with those for electronic processes. Consequently, the neutral component at angles larger than 1° is taken to be H^0 alone.

Several sources of error are present in each of the measured quantities and have been discussed in previous papers.^{1,5} These involve the effective length of the interaction cell, the angular resolution, and the detector calibration. Although data were corrected to account for most of these uncertainties, a total error of $\pm 20\%$ in the final data has been estimated.

III. THEORY OF THE ANGULAR DISTRIBUTIONS

A theory of fragment angular distributions was derived in Ref. 1 for the case of a homonuclear binary molecule excited to a dissociating state in a collision with a target. Although Ref. 1 referred specifically to the electron-capture processes, the results therein derived are also valid for direct excitation. The theory was later generalized to nonhomonuclear binary molecules incident on a target,¹¹ but the generalization is not needed here and will not be further discussed. The theory of Ref. 1 is based on five assumptions, all valid in the present experiment.

(i) The electronic process is fast compared with the periods of both vibrational and rotational motion. The incident molecule can therefore be considered to have a fixed orientation and a fixed geometry during the excitation process.

(ii) Rotational energies are negligible compared with dissociation energies, so that the dissociation direction is that of the line joining the two fragments.

(iii) All orientations are equally probable.

(iv) Dissociation velocities are small compared with incident-beam velocities.

(v) The center of mass of the molecular ion suffers a negligible deflection due to the electronic excitation.

Thus the angular difference between the direction of motion of a fragment and the incident-beam direction is due entirely to the transverse component of the velocity of the dissociating fragments.

Based on these assumptions, it was shown in Ref. 1 that the angular distribution $d\sigma_i/d\omega$ of dissociation fragment i as a function of laboratory angle θ is given by

$$\frac{1}{E_{\text{inc}}} \frac{d\sigma_a}{d\omega} = \frac{1}{E_{\text{inc}}} \frac{d\sigma_b}{d\omega} = \frac{1}{4\pi} \int_0^{R_d} \frac{\sigma_{g-ab}(R, \Theta, E_{\text{inc}}) \rho(R) dR}{[E_d^{ab}(E_d^{ab} - E_{\text{inc}} \theta^2)]^{1/2}} \quad (3)$$

In Eq. (3), σ_{g-ab} is the total cross section for

collisional excitation from the ground state, designated by g , to the repulsive state labeled by the double index ab indicating the two fragments into which the state dissociates. Thus $0, +1$ indicates the directly excited repulsive state of H_2^+ , while $0, 0$ indicates the repulsive state of H_2^0 formed by electron capture. The cross section σ is a function of the proton-proton separation R and its orientation Θ relative to the beam direction at the time of collision. In general, it will also depend on the incident energy. The azimuthal angle ϕ is unobservable and has averaged over. The dissociation energy E_d is a function of R and also depends on the particular repulsive state involved. Finally, $\rho(R)$ gives the distribution of proton-proton separations, E_{inc} is the incident H_2^+ energy in the laboratory frame, and R_d is the value of R for which $E_d = E_{\text{inc}} \theta^2$. It was shown in Ref. 1 that for small angles θ , $\cos \Theta \approx [(E_d^{ab} - E_{\text{inc}} \theta^2)/E_d^{ab}]^{1/2}$, so that Θ is a function of R (which is integrated over) and $E_{\text{inc}} \theta^2$ only. Since R_d is also

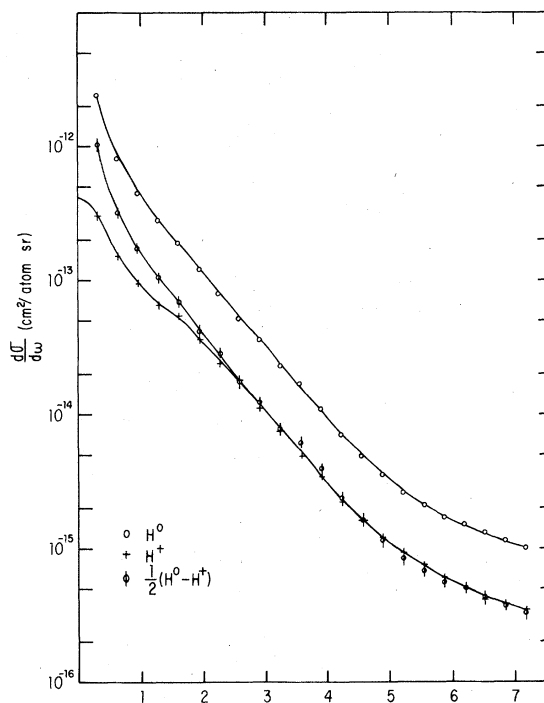


FIG. 2. Typical angular distributions of dissociation fragments measured at 2 keV incident H_2^+ projectile energy in collisions with He. The angle θ gives the laboratory angle with respect to the incident beam direction at which the fragment was detected. The H^+ distribution arises from direct excitation of the incident H_2^+ ion to the repulsive $1\sigma_u$ state. The curve labeled $\frac{1}{2}(H^0 - H^+)$ gives the angular distribution of H^0 which arises from electron capture from the target He to the $^3\Sigma_u$ repulsive state of H_2^0 .

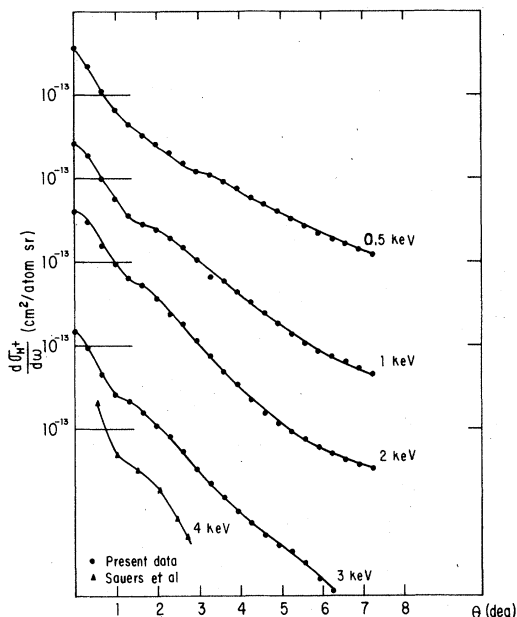


FIG. 3. Angular distributions for the formation of H^+ fragments in collisions of 0.5, 1.0, 2.0, and 3.0 keV H_2^+ projectiles incident on He target gas. Here θ is the laboratory angle with respect to the incident-beam direction at which the fragment was detected. The data of Sauers *et al.* (Ref. 4) at 4.0 keV are included for comparison. Each division on the vertical axis represents an order of magnitude. The horizontal bar marked 10^{-13} establishes the 10^{-13} level for the curve which it intersects. Thus, the second bar from the top represents 10^{-13} for the 1.0 keV curve, but 10^{-14} for the 0.5 keV curve.

a function of $E_{inc} \theta^2$, the entire integral in (3) is a function of the scaled variable $E_{inc} \theta^2$ and the repulsive state involved only, if the excitation cross section does not depend on incident energy. It is seen from Eq. (3) that the angular distributions for both dissociation fragments are identical and that for any process $g \rightarrow ab$, if $(1/E_{inc}) d\sigma/d\omega$ is plotted as a function of $E_{inc} \theta^2$, the results for all incident energies will lie on a universal curve:

$$(1/E_{inc})d\sigma/d\omega = f_{ab}(E_{inc} \theta^2). \quad (4)$$

If the excitation cross section does depend on collision energy, but only as a multiplicative factor,

$$\sigma_{ab}(R, \theta, E_{inc}) = g(R, \theta) N(E_{inc}), \quad (5)$$

then the scaled angular distributions will be identical in shape differing only by a "normalization" factor:

$$(1/E_{inc})d\sigma/d\omega = N(E_{inc}) f_{ab}(E_{inc} \theta^2). \quad (6)$$

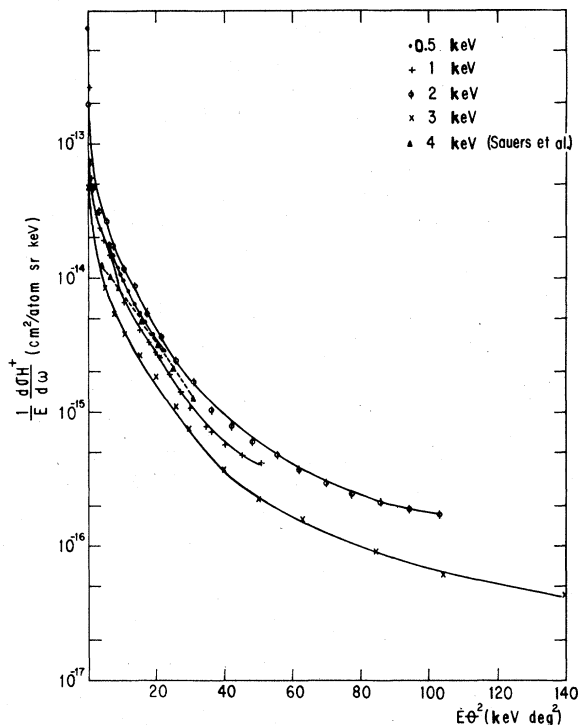


FIG. 4. The angular distributions of Fig. 3 replotted in terms of the reduced variables $(1/E)d\sigma/d\omega$ and $E\theta^2$ of Ref. 8, where E is the incident projectile energy in the laboratory frame.

IV. EXPERIMENTAL RESULTS AND INTERPRETATIONS

A. The experimental data

Figure 2 illustrates typical data for the angular distributions of dissociation fragments when H_2^+ is incident on He. In Fig. 2, the collision energy is 2 keV. Three distributions are shown: for H^+ , H^0 , and $\frac{1}{2}(H^0 - H^+)$. The H^+ ions come from the dissociation of H_2^+ directly excited to the $1\sigma_u$ repulsive state. For every H^+ ion found at angle θ with respect to the incident-beam direction, there will also be an H^0 at the same angle. Thus, to obtain the number of H^0 which arose from the dissociation of H_2^0 , it is necessary to subtract the number of H^+ from the number of H^0 at each angle. Then, since each H_2^0 dissociation produces two H^0 , it is necessary to divide the number of $H^0 - H^+$ by 2. Figure 3 shows the angular distributions of H^+ fragments at 0.5, 1.0, 2.0, and 3.0 keV incident energy, along with the data of Sauers *et al.*⁴ at 4 keV. These angular distributions are replotted in Fig. 4 in terms of the reduced variables $(1/E_{inc})d\sigma/d\omega$ and $E_{inc} \theta^2$, the curves obtained from the 0.5, 1.0, 2.0, and 3.0-keV data of the present work are seen to be similar in shape. A constant multiple of each curve will bring them

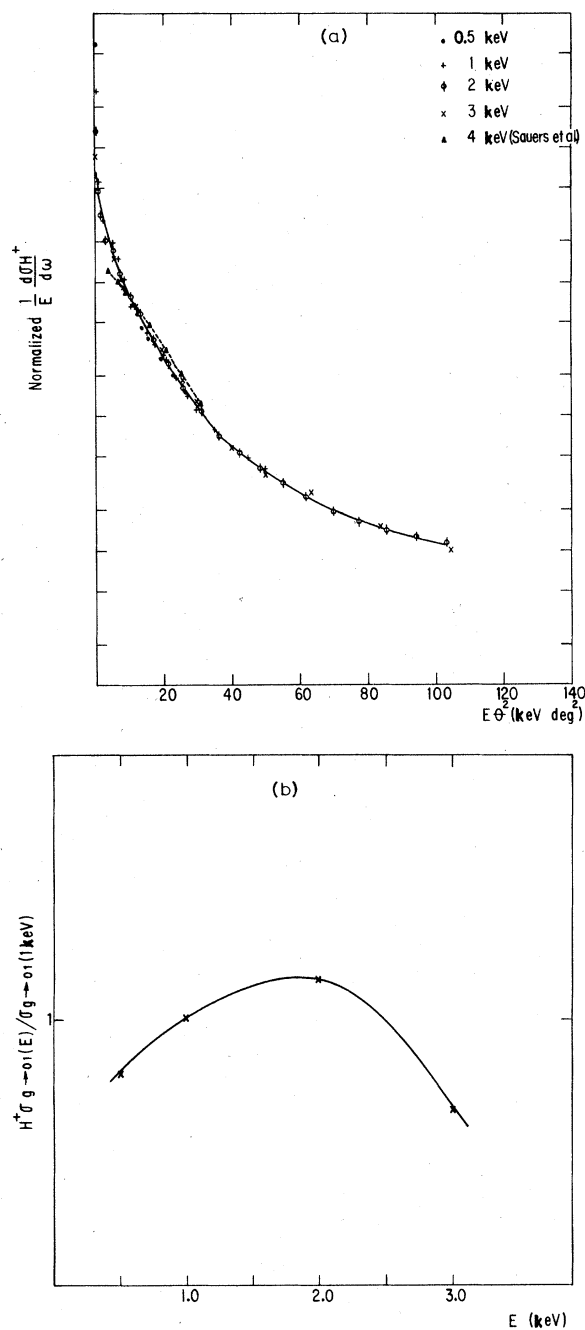


FIG. 5. (a) The four reduced angular distributions at 0.5, 1.0, 2.0, and 3.0 keV in Fig. 4 multiplied by different "normalization" constants. (b) The reciprocals of these normalization constants give the energy dependence for the direct excitation cross section $H_2^+(1\sigma_g) \rightarrow H_2^+(1\sigma_u)$, in terms of the cross section at 1 keV.

all into a single universal distribution except at small angles. This is seen in Fig. 5(a). The universal H^+ distribution indicates that the $1\sigma_g \rightarrow 1\sigma_u$ direct excitation cross section has an inci-

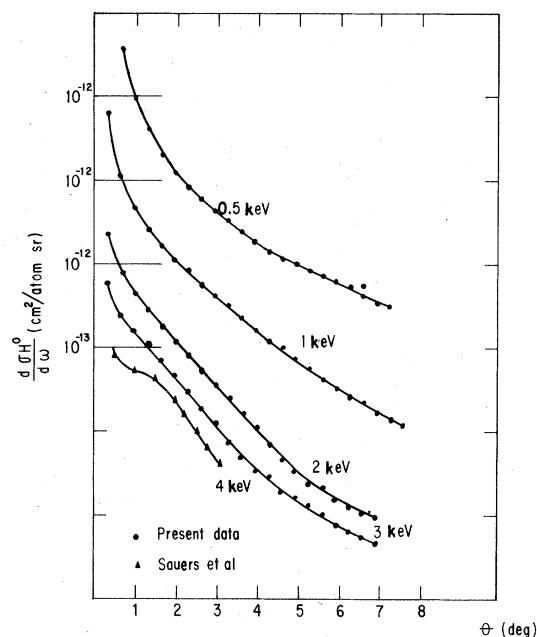


FIG. 6. Angular distributions for H^0 fragments from collisions of H_2^+ on He at collision energies 0.5, 1.0, 2.0, and 3.0 keV incident energy. The data of Sauer *et al.* at 4.0 keV are included for comparison. Each division on the vertical axis represents an order of magnitude. The second bar from the top represents 10^{-12} for the 1.0 keV curve, but 10^{-13} for the 0.5 keV curve. The bottom three curves (2.0, 3.0, and 4.0 keV) are all on the same scale with 10^{-12} determined by the horizontal bar which intersects the 2.0 keV curve.

dent energy (i.e., velocity) dependence of the type described in Eq. (5). The reciprocals of the normalization constants give the energy dependence of the excitation cross section and are presented in Fig. 5(b).

Figure 6 shows the H^0 dissociation fragment angular distributions at 0.5, 1.0, 2.0, and 3.0 keV incident energy along with the 4-keV data of Sauer *et al.*⁴ Figure 7 shows the angular distributions for $\frac{1}{2}(H^0 - H^+)$, which arise from dissociation of the $H_2^0(^3\Sigma_u)$ state. (It was not possible to read the data of Sauer *et al.* with sufficient accuracy to include in Fig. 7). The "normalized" distributions of Fig. 7 are shown in Fig. 8(a) which indicates that cross section for the $H_2^+(1\sigma_g) \rightarrow H_2^0(^3\Sigma_u)$ charge-exchange collision also has a velocity dependence of the type described by Eq. (5). The reciprocals of the normalization constants give the energy dependence of cross section and are presented in Fig. 8(b).

B. Interpretation of the experimental results

In an earlier experiment similar to the present one, Sauer *et al.*⁴ measured angular distributions

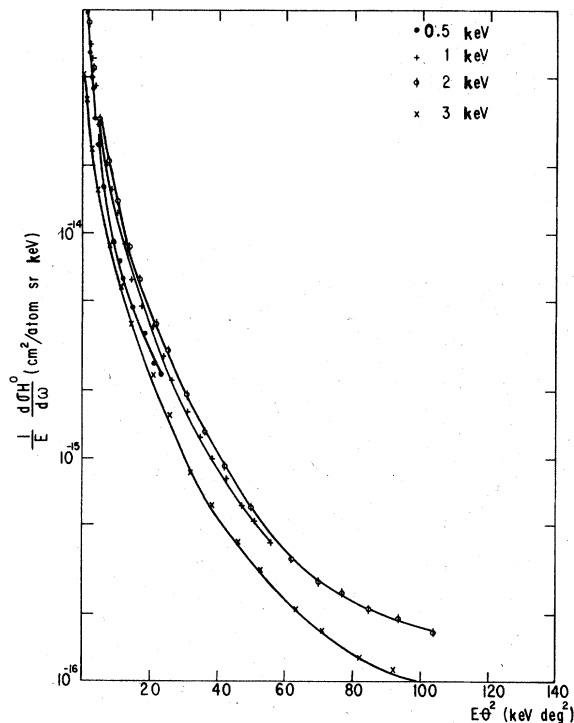


FIG. 7. The angular distributions for the combination $\frac{1}{2}(H^0 - H^+)$ plotted in terms of the reduced variables $(1/E)d\sigma/d\omega$ and $E\theta^2$ of Ref. 8, where E is the incident projectile energy in the laboratory frame. The combination $\frac{1}{2}(H^0 - H^+)$ gives the angular distribution of H^0 fragments which arise from electron capture by the incident ground state H_2^+ into the ${}^3\Sigma_u^0$ repulsive state of H_2^0 .

of H^+ and H^0 dissociation fragments from H_2^+ on He collisions, but at higher collision energies. The lowest energy data of Sauer *et al.* (at 4 keV) is included along with the data of the present experiment for comparison. It can be seen from Figs. 3, 4, and 6 that the angular distributions of the two experiments are in reasonable agreement. In fact, the difference between the scaled H^+ distributions, compared in Fig. 4, is probably *not* due to experimental discrepancy; more likely, it is a real physical effect. Gibson *et al.*³ found a sharp onset of higher dissociation energies going from 3 keV collision energy to 5 keV, which they attributed to the onset of a second excitation process. That is precisely what the data of Sauer *et al.* at 4 keV indicate. Roughly speaking, $E\theta^2$, with θ measured in radians, gives the dissociation energy. (More precisely, it is equal to the dissociation energy for those dissociations in which the H_2^+ was oriented perpendicular to its direction of motion at the time of excitation). The 4-keV data thus show a larger number of higher dissociation energies.

Insofar as the H^+ angular distributions are con-

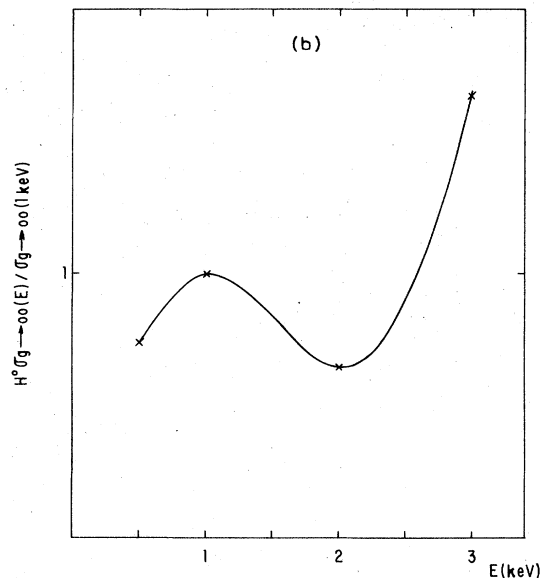
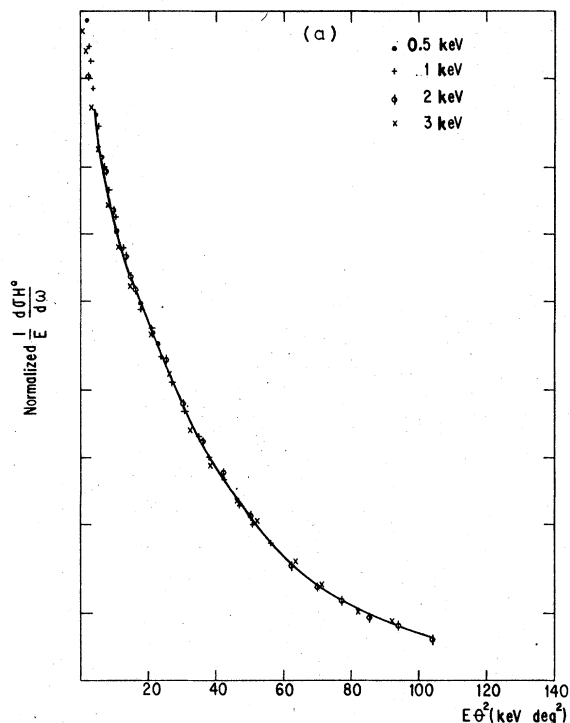


FIG. 8. (a) The four angular distributions of Fig. 7 multiplied by different "normalization" constants. (b) The reciprocals of these normalization constants give the energy dependence of the cross section for the charge-exchange process $H_2^+(1\sigma g) + He(1s^2) \rightarrow H_2^0({}^3\Sigma_u) + He^+(1s)$ in terms of the cross section at 1 keV.

cerned, a comparison can be made with the results of Gibson, Los, and Schopman,³ which this work partly overlaps and partly complements. The experiment of Gibson *et al.* directly provides the dependence on R and Θ of the relative excita-

tion cross section σ_{g-01} for H_2^+ on He at collision energies 3.0, 5.0, 7.5, and 10.0 keV. They found going from 3 keV up to 10 keV the R dependence of σ_{g-01} changes dramatically, which they attributed to the onset of a second excitation process. The present experiment conclusively demonstrates that from 3 keV down to 0.5 keV, the dependence of σ_{g-01} on R and Θ does not change. Although it is not feasible to invert Eq. (3) to obtain $\sigma_{g-01}(R, \Theta)$ from the reduced angular distribution of Fig. 5(a), the angular distribution for small and moderate $E\theta^2$ of Fig. 5(a) is generally consistent with the functional form for σ_{g-01} found by Gibson *et al.* at 3 keV. A significant difference, however, is found at higher values of $E\theta^2$. Gibson *et al.* obtain a dependence of σ_{g-01} on R in atomic units very nearly described by $A(R-1.4)$ for $R > 1.4$ and 0 for $R < 1.4$ a.u. Such an R dependence would make the distribution of Fig. 5(a) fall to zero at $E\theta^2 \approx 55$ keV deg², which is clearly not the case. Thus, the present experiment finds evidence that the R dependence of σ_{g-01} does not vanish unless $R \sim 0.9$ a.u.

Gibson *et al.* found qualitative agreement at 10 keV collision energy between their experimental determinations of $\sigma_{g-01}(R, \Theta)$ for H_2^+ on He and the Born approximation calculations of Green and Peek.¹² They also found a second process to occur in the restricted range $E_{inc} \geq 5$ keV, small R , and $\theta \approx 90^\circ$. They attributed this second process to simultaneous excitation of the incident H_2^+ and the target atom, and concluded that it did not fit the Born approximation predictions. The present results indicate that: (1) The R and Θ dependence of σ_{g-01} is unchanged from 3 keV down to 0.5 keV; and (2) the second process may not, in fact, be restricted to $E_{inc} \geq 5$ keV, but may occur at all energies down to 0.5 keV.

ACKNOWLEDGMENT

This work was partially supported by joint Grant Nos. NSF-PNCB-CONACyT 1367 and PCCBNAL 790086.

¹C. Cisneros, I. Alvarez, C. F. Barnett, J. A. Ray, and A. Russek, *Phys. Rev. A* **14**, 88 (1976).

²D. K. Gibson and J. Los, *Physica (Utrecht)* **35**, 258 (1967).

³D. K. Gibson, J. Los, and J. Schopman, *Physica (Utrecht)* **40**, 385 (1968).

⁴I. Sauers, R. L. Fitzwilson, J. C. Ford, and E. W. Thomas, *Phys. Rev. A* **6**, 1418 (1972).

⁵C. Cisneros, I. Alvarez, C. F. Barnett, and J. A. Ray, *Phys. Rev. A* **14**, 76 (1976).

⁶L. Wahlin, *Nucl. Instrum. Methods* **27**, 55 (1964).

⁷J. A. Ray (private communication).

⁸H. H. Fleischmann, C. F. Barnett, and J. A. Ray, *Phys. Rev. A* **10**, 569 (1974).

⁹G. A. Harrower, *Rev. Sci. Instrum.* **26**, 850 (1955).

¹⁰D. H. Crandall, J. A. Ray, and C. Cisneros, *Rev. Sci. Instrum.* **46**, 562 (1975).

¹¹C. Cisneros, I. Alvarez, R. García G., C. F. Barnett, J. A. Ray, and A. Russek, *Phys. Rev. A* **19**, 631 (1979).

¹²T. A. Green and J. M. Peek, *Phys. Rev.* **183**, 166 (1969).